Contemporary Engineering Sciences, Vol. 8, 2015, no. 13, 549 - 555
HIKARI Ltd, www.m-hikari.com
http://dx.doi.org/10.12988/ces.2015.54140

Strength and Dissipated Energy of Steel Fiber Reinforced Concrete Link Beams

Sun-Woong Kim

Department of Convergence Systems Engineering, Chungnam National University, 99 Daehak-ro Yuseong-gu, Daejeon, 305-764, Republic of Korea

Young-Il Jang

Department of Construction Engineering Education, Chungnam National University, 99 Daehak-ro Yuseong-gu, Daejeon, 305-764
Republic of Korea

Wan-Shin Park

Department of Construction Engineering Education, Chungnam National University, 99 Daehak-ro Yuseong-gu, Daejeon, 305-764, Republic of Korea
Corresponding author

Nam-Yong Eom

Department of Technology Education, Chungnam National University
99 Daehak-ro Yuseong-gu, Daejeon, 305-764, Republic of Korea

Hyun-Do Yun

Department of Architectural Engineering, Chungnam National University
99 Daehak-ro, Yuseong-gu, Daejeon, 305-764, Republic of Korea
Corresponding author

Sun-Woo Kim

Department of Construction Engineering Education, Chungnam National University, 99 Daehak-ro Yuseong-gu, Daejeon, 305-764, Republic of Korea

Abstract

This aim of this study is to investigate the strength and dissipated energy of steel fiber-reinforced concrete (SFRC) link beam as an innovative method of improving the seismic performance of reinforced concrete link beam. Experiments were conducted for three link beams. Two out of them were strengthened by steel fiber for reinforced concrete of link beam and the other one was selected as a control specimen without strengthening. Based on the observation of test results, the shear capacity of steel fiber reinforced link beams were improved in comparison to reinforced concrete link beam without steel fiber.

Keywords: Steel Fiber, Link Beam, Strain Characteristics, Reinforced Concrete

1 Introduction

Link beams are very efficient structures as the walls play dual function. In addition link beams are used to connect individual wall piers in coupled shear walls as efficient lateral-force-resisting systems with large strength and dissipation energy [1]. Steel fiber reinforced concrete (SFRC) has been widely used in construction sites [2,3]. In addition SFRC, randomly oriented discontinuous in cementite's materials reduces the level of micro-cracking and enhances the toughness, ductility, energy dissipation and post-cracking tensile resistance of concrete members [4-6]. In this work to quantify the improvement in behavior of reinforced concrete link beams upon adding steel fibers compared to control specimens without fibers in a series of experiments. To provide recommendations were to practicing engineers and allow them greater flexibility in design.

Table. 1 Test Variable

Specimen name	Reinforcement method	Material	Longitudinal reinforcement	Leg bar	Fiber Volume (%)
C-1	Diagonal reinforcement + leg bar	Concrete	12D-6	D6@50	-
C-2	Diagonal reinforcement + Steel fiber	SFRC	12D-6	D6@200	1.5
C-3	Diagonal reinforcement	Concrete	12D-6	D6@200	-

2 Experimental Programs

Table 1 and Figure 1 show the test variables and specimen details. These three specimens have identical dimensions and longitudinal reinforcement details. Test variables of this study are types of materials, leg bars and connection details in steel fiber reinforced link beam shear wall connection region.

Tests were taken to determine actual properties for compressive strength of concrete and SFRC, tensile strength of SFRC and steel reinforcement. Figure 2 shows the test results of mechanical properties for concrete, SFRC and steel. The concrete and SFRC compressive strength was approximately 68MPa and 60MPa respectively, as shown the Fig. 2 (a). The flexural strength of SFRC material under monotonic load is about 3.3MPa, as shown in Fig. 2(b).

The test setup is shown in detail in Fig. 3. A hydraulic actuator with a capacity of 1000 kN is fixed to the reaction wall. It is then able to exert forces onto the top steel girder in both positive and negative directions. Instrumentation was provided to measure the load, displacement, and strain at critical locations. The displacement of all the specimens was controlled to follow similar displacement histories with progressively increasing amplitude.

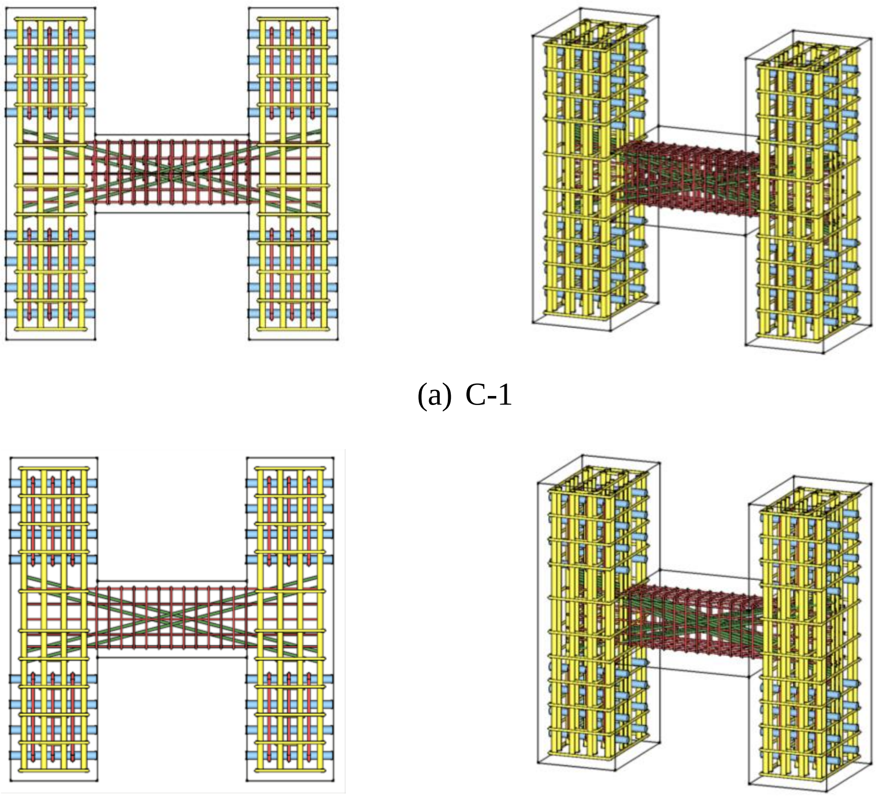

(a) C-1

(b) C-2 & C-3

Fig. 1 Details of specimens

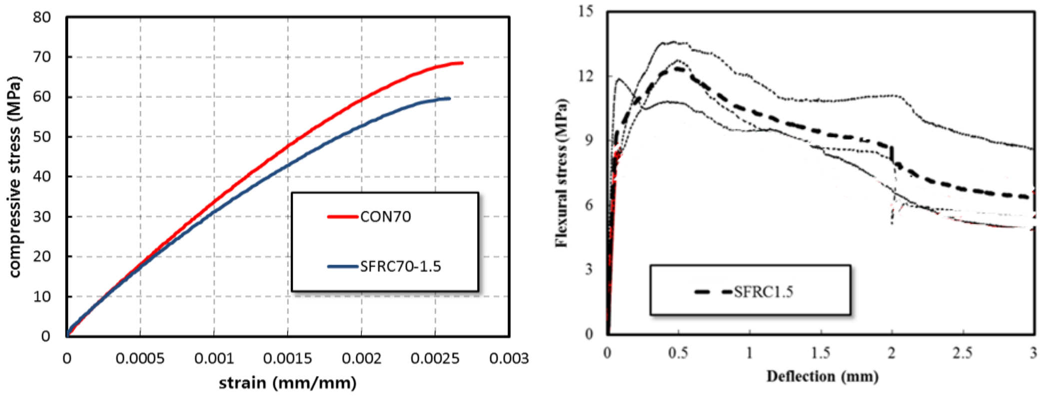

(a) Compressive strength (b) Flexural strength for SFRC

Fig. 2 Mechanical properties

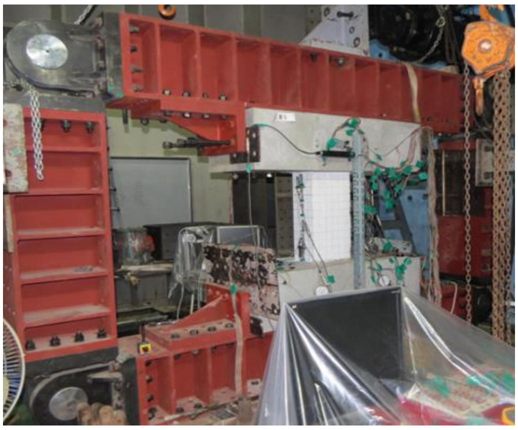

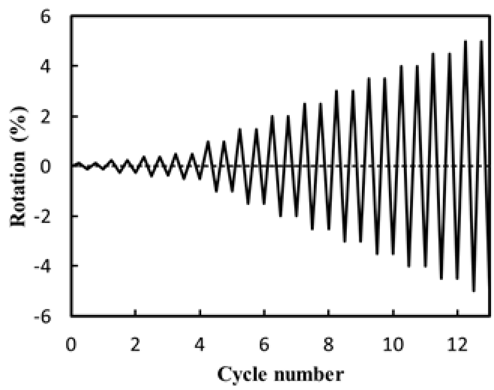

Fig. 3 Test set-up

Fig. 4 Loading History

The data acquisition system consists of 20 to 36 internal controls and recording channels. Instrumentation was provided to measure the load, displacement, and strain at critical locations. The testing procedure included load-controlled and displacement-controlled cycles, as shown in Fig. 4.

3 Experimental Results

Table 2 and Figure 5 show the maximum strengths and the hysteretic response plotted against the displacement. As listed in Table 2, the first specimen C-1 reached its peak load of 412.61kN in the positive loading direction and 408.40kN in the negative loading direction. The second specimen C-2 reached its peak load of 475.69kN in the positive loading direction and 473.26kN in the negative loading direction. The third specimen C-3 reached its peak load of 379.90kN in the positive loading direction and 393.33kN in the negative loading direction. The average maximum strength of specimens C-1, C-2 and C-3 were 410.51kN, 474.48kN and 386.62kN respectively. In addition, average maximum strength of C-2 specimen is 1.15 and 1.23 times higher than those of specimens C-1 and C-3, respectively.

Figure 5 (a) to (c) give load-deflection curves of the three specimens tested. Definitions of the positive direction of the applied load and the deflection were depicted by a legend in each figure. Two specimens C-1 and C-2 did exhibit any stable spindle-type hysteretic loops. However C-3 specimen did not exhibit any stable spindle-type hysteretic loop. As shown in Figure 5 (a), C-1 specimen sudden decreases in strength during the first and second cycles at a displacement of about 24mm. This is attributed to the effect of the localized spalling and crushing of the concrete along the bottom surface of the link beam. As shown in Figure 5 (b), C-2 specimen did stable spindle hysteretic loops during the all cycle end of the test. This is attributed to the bridging action of steel fiber by using the instead of concrete. C-3 specimen showed sudden decrease in strength beyond the maximum strength as shown in Fig. 5(c). This is attributed to the premature buckling of the diagonal bars.

A graph of the cumulative dissipated energy is plotted in Fig. 6. At a first number of cycle 1 (0.5% rotational angle), cumulative dissipated energy for specimens C-1, C-2 and C-3 values were equal to 1.18 kN·m, 0.98 kN·m and 0.94 kN·m, respectively. For the number of cycle 8 (4% rotational angle), the cumulative dissipated energy of specimen C-1 was 101% and 143% larger than that of specimens C-2 and C-3, respectively. In addition, the cumulative dissipated energy of specimen C-2 at failure was 143% and 251% larger than that of specimens C-1 and C-3, respectively.

The results in Figure 6 show that in spite of slightly higher performance of C-2 specimen in dissipating the energy during the loading process, increasing of number of cycle indeed does improve the energy dissipation capability of the C-1 and C-3.

Table. 2 Maximum strength

Specimen	Maximum strength		
	Positive loading	Negative loading	Average maximum strength
C-1	412.61kN	408.40kN	410.51kN
C-2	475.69kN	473.26kN	474.48kN
C-3	379.90kN	393.33kN	386.62kN

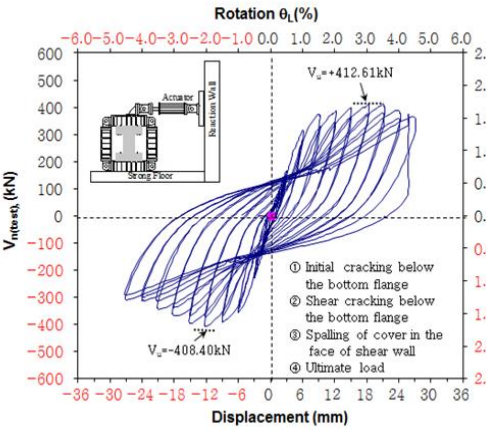

(a) Specimen C-1

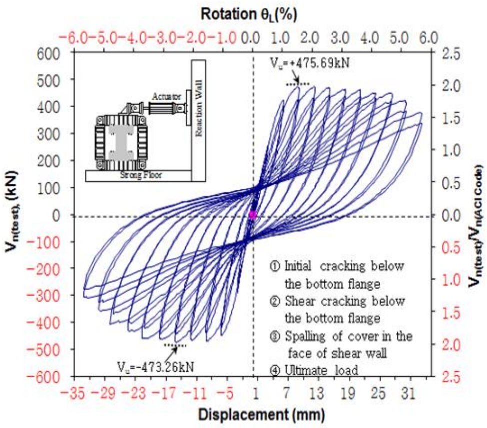

(b) Specimen C-2

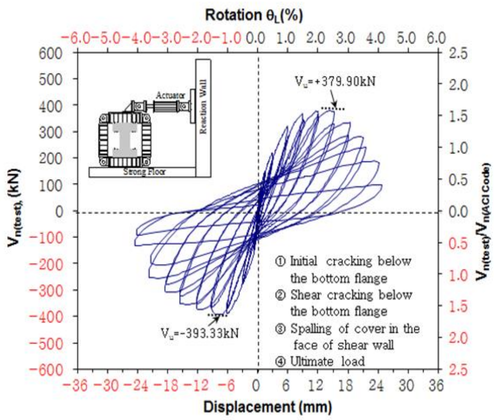

(c) Specimen C-3

Fig. 5 Hysteretic loop

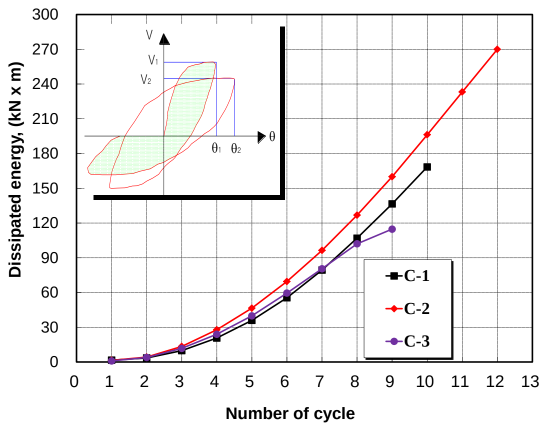

Fig. 6 Dissipated energy

4. Conclusion

Base on the observation of test results, the average maximum strength of specimens C-1, C-2 and C-3 were 410.51kN, 474.48kN and 386.62kN respectively. In addition, average maximum strength of C-2 specimen is 1.15 and 1.23 times higher than those of specimens C-1 and C-3, respectively. The second, two specimens C-1 and C-2 did exhibit any stable spindle-type hysteretic loops. However C-3 specimen did not exhibit any stable spindle-type hysteretic loop. The third, C-2 specimen in dissipating the energy during the loading process, increasing of number of cycle indeed does improve the energy dissipation capability of the C-1 and C-3.

Acknowledgements. This research was supported by Basic Science Research Program through the National Research Foundation of Korea (NRF) funded by the Ministry of Science, ICT & Future Planning (2014R1A1A2057931) and This work was supported by research fund of 2014 Chungnam National University (2014-0756).

References

[1] Wan-Shin Park, Hyun-Do Yun, Seismic behaviour of steel coupling beams linking reinforced concrete shear walls, *Engineering Structures*, Vol. 27, No. 9, (2005), pp. 1024-1039. http://dx.doi.org/10.1016/j.engstruct.2005.02.013

[2] Sharma A. K., Shear Strength of Steel Fiber Reinforced Concrete Beams, *ACI Journal*, Vol. 83, No. 4, (1986), pp. 624-628. http://dx.doi.org/10.14359/10559

[3] Ashour S. A., Hasanain G. S. and Wafa F. F., Shear Behavior of High-Strength Fiber Reinforced Concrete Beams, *ACI Structural Journal*, Vol. 89, No. 2, (1992), pp. 176-184. http://dx.doi.org/10.14359/2946

[4] Khuntia M., Bozidar S. and Subhash C. G., Shear Strength of Normal and High –Strength Fiber Reinforced Concrete Beams without Strirrups, ACI Structural Journal, Vol. 96, No. 31, (1999), pp. 282-289. http://dx.doi.org/10.14359/620

[5] Wan-Shin Park, Hyun-Do Yun, Bearing Strength of Steel Coupling Beam Connections embedded Reinforced Concrete Shear Wall, *Journal of Engineering Structures*, Vol. 28, No. 9, (2006), pp. 1319-1334. http://dx.doi.org/10.1016/j.engstruct.2006.01.003

[6] Wan-Shin Park, Hyun-Do Yun, Seismic Performance of Pseudo Strain-Hardening Cementitious Composite Coupling Beams with Different Reinforcement Details, *Composite: Part B*, Vol. 42, No. 6, (2011), pp. 1427-1445. http://dx.doi.org/10.1016/j.compositesb.2011.04.049

Received: April 16, 2015; Published: May 29, 2015